Parametrization of turbulent form drag due to the smallest-scale unresolved orography

Laura Rontu, Finnish Meterological Institute
laura rontu@fmi.fi

1 Introduction

In a NWP model the tendencies of the horizontal wind $\vec{v}(x, y, z)$ are explicitly resolved (index d) or parametrized (index p):

$$\frac{\partial \vec{v}}{\partial t} = (\frac{\partial \vec{v}}{\partial t})_d + (\frac{\partial \vec{v}}{\partial t})_p \tag{1}$$

The parametrized tendency is due to the divergence of the stress tensor τ_{ij}. In practice, only the vertical component is included into the parametrizations.

$$(\frac{\partial \vec{v}}{\partial t})_p = \frac{1}{\rho}\frac{\partial \vec{\tau}}{\partial z}, \tag{2}$$

where $\vec{\tau} = -\sum_{j=1}^{n} \rho(\overline{\vec{v}' w'})_j$ and the index j refers to different subgrid-scale processes.

The subgrid-scale momentum fluxes can be divided into components due to surface friction, small-scale turbulent form drag and buoyancy (gravity) waves:

$$\vec{\tau}_{total} = \vec{\tau}_{friction} + \vec{\tau}_{formdrag} + \vec{\tau}_{wave} \tag{3}$$

With increasing horizontal scale and stability wave-related processess gain more influence while turbulent processess of surface friction and small-scale form drag are more important in the smallest scale and moderately stable stratification.

The present and suggested parametrizations in HIRLAM are shown in Table 1. In the following we concentrate on the parametrization of small-scale turbulent form drag which will be referred to as small-scale orography (SSO) drag.

HIRLAM	stress	now	then
	$\vec{\tau}_{friction}$	$z_{o,veg}$	$z_{o,veg}$
	$\vec{\tau}_{formdrag}$	$z_{o,veg} + z_{o,oro}$	SSO parametrization
	$\vec{\tau}_{wave}$	-	MSO parametrization

2 Parametrization of the small-scale turbulent form drag

Form (pressure) drag due to small-scale orographic features is related to the process of non-separated sheltering (Belcher et al., 1993), which creates a pressure distribution with lower pressure over the lee side of the obstacle. This is entirely a property of viscous, turbulent flow while the buoyancy waves (mountain lee waves) exist in adiabatic, frictionless flow also. Strafication from neutral to moderately stable and orography scales below a few kilometres create favourable conditions for the SSO drag. An additional contribution to the form drag may be given by flow separation and wakes, which are not included in the parametrizations considered here.

According to Wood and Mason (1993); Wood et al. (2001) the SSO drag can be expressed as

$$\vec{\tau}_{sso}(z=0) = \rho\alpha\beta\theta^2 u_{*o}^2 \gamma, \tag{4}$$

where

ρ	=	air density
α	=	shear-dependent factor
β	=	anisotropy 0...1
θ	=	maximum slope of orography (tangent)
u_{*o}	=	undisturbed friction velocity
γ	=	function of direction 0...1

In the present NWP the subgrid-scale orographic drag is most often handled with the concept of orographic roughness introduced by Mason (1985). Here, the small-scale orography effects are included into the surface layer parametrizations in analogy to the surface friction. An effective friction velocity $u_{*,eff} = \sqrt{|\vec{\tau}_{eff}|/\rho}$ is assumed to consist of an undisturbed (u_{*o}) and an orographic ($u_{*,oro}$) component:

$$u_{*,eff}^2 = u_{*o}^2 + u_{*,oro}^2 \tag{5}$$

An effective roughness length $z_{o,eff}$ is based on the experimental result that a logarithmic wind profile is valid over large areas and in depths comparable to the vertical scale of the underlying orography:

$$u = \frac{u_{*,eff}}{z} log \frac{z}{z_{o,eff}} \tag{6}$$

The orographic roughness giving rise to $u_{*,oro}$ is parametrized based on variations of subgrid-scale slopes according to Eq. (4). The effective roughness, which consists of components due to the surface properties ($z_{o,veg}$, local or vegetation roughness) and orography ($z_{o,oro}$), can now be derived from Eqs. (6) and (5), based on observations and experimentation. Further, the values of effective or orographic roughness are introduced into the surface layer parametrizations instead of or in addition to the conventional roughness lenght. In practice, the orographic roughness has evolved from these first principles towards a tuning parameter, whose values are pragmatically modified in order to improve the behaviour of each particular NWP model (also HIRLAM).

Wood et al. (2001), see also Wilson (2003), suggested a new approach to SSO parametrization. Instead of the indirect method involving surface layer similarity theory, the SSO drag is calculated directly from Eq. (4) and used to modify the wind component values. It is further assumed that the vertical structure of the stress vector can be expressed with a simple exponential profile

$$\vec{\tau}_{sso}(z) = \vec{\tau}_{sso}(z=0) exp(-z/l_{sso}), \tag{7}$$

where l_{sso} is a suitable length scale. The values of $\tau_{sso} = \vec{\tau}_{formdrag}$ can now be used in Eqs (1)-(3) to give the tendencies of wind components due to the small-scale orography effects.

The suggested method is simpler and more transparent than the method of effective (orographic) roughness. The drag is not restricted to the surface layer but has a three-dimensional structure. However, there may be different ways to define the length scale related to the vertical structure (Eq. 7). Separation of the momentum and scalar (heat and humidity) fluxes follows automatically as the SSO parametrizations only effect the former. Influence of the surface layer stratification enters through the undisturbed friction velocity (Eq. 4), where the turbulent drag coefficients depend on stability (for HIRLAM formulations, see Undén et al. (2002)). In case of unstable stratification this might be not entirely correct and may need further modification. Introduction of direction and anisotropy effects is straight-forward (Wood et al., 2001; Brown and Wood, 2001). The suggested formulations are similar to those used in buoyancy wave parametrizations and thus bring these two approaches closer to each other.

3 HIRLAM application

The specific features of the HIRLAM SSO parametrization based on Wood et al. (2001) include:

- Only orography scales smaller than 3 - 4 km kilometres contribute to the SSO drag. The slope parameter θ is defined as mean maximum SSO slope over a grid-square and calculated from one-kilometer resolution orography data (http://edcdaac.usgs.gov/gtopo30/hydro/) with aggregation to the model grid of needed resolution. Details of the calculation are given in (Rontu, 2003). (In the new SSO parametrization of ECMWF by Beljaars et al. (2004), a more general and sophisticated spectral approach to the representation of underlying small-scale orography variations is adopted. The practical importance of this complication remains to be verified.)

- SSO parametrization is applied together with a mesoscale orography (MSO) parametrization (Rontu et al., 2002), representing the effects due to the orography scales between a few kilometres and two-three grid-lengths.

- Anisotropy and direction effects are not taken into account. It is assumed that the smallest-scale features contributing to the SSO drag are sufficiently isotropic. Thus, coefficients β and γ equal unity in Eq. (4).

- In Eq. (4) the value of the coefficient α is defined based on model experiments. According to Wood et al. (2001), $|\tau_{o,oro}| \approx 20\% \, |\tau_{o,veg}|$ for slopes $\approx$ 10 deg. As a result of smoothing over possibly large areas, the mean maximum slopes within a grid-square are typically only a few degrees. This might be compensated by increasing the value of α with decreasing model resolution. The smallest-scale orography standard deviation σ_{sso} is taken to represent the length scale l_{sso}.

4 HIRLAM experiments

A series of 11-day HIRLAM experiments (19-29 January, 2000) were run in order to compare the subgrid-scale parametrizations related to the momentum fluxes. Table 1 gives the definition of the experiments. The code was based on the HIRLAM reference version 6.3.3 with some technical corrections. In the experiments, a European area with a resolution of Δx=33 km/40 levels was used. The +48h forcasts were started at 00 UTC, otherwise a data-assimilation cycle of 6h was maintained. Boundaries were given by a FMI HIRLAM reanalysis for the year 2000, which has been run at ECMWF with HIRLAM 6.2.2, 33 km/40 levels. Observations were taken from the ECMWF archive.

Table 1: Definition of the numerical experiments

experiment	description
RC33	reference HIRLAM with technical corrections
NO33	RC33 but SSO parametrization instead of $z_{oro,0}$
NM33	NO33 but MSO parametrization added
NT33	NM33 but with rotated turbulent stress vector and related modifications in turbulence scheme

Results of the standard verification statistics over EWGLAM stations are shown in Fig. 1. Based on the verification of the ten-metre wind it can be concluded, that the SSO parametrizations alone are not sufficient to replace the enhanced orographic roughness used in the reference HIRLAM. When MSO parametrizations are added, the ten-metre wind verification is improved to give the same result as the reference, but a slight positive surface pressure bias appears. After combining the new SSO and MSO parametrizations with a suggested modification of the direction of the turbulent surface stress (Sass and Nielsen, 2004) the wind bias is halved. This indicates the important role of the basic turbulence parametrizations in model's surface layer and above.

Fig. 2 depicts vertical profiles of tendencies of resolved-scale kinetic energy due to different parametrized processes, averaged over time and Scandinavian area. The change of kinetic energy k equals the work done by frictional forces (parametrized turbulence, SSO and MSO effects). It can be estimated as follows, based on the values of wind components and their accumulated tendencies:

$$(\frac{\partial k}{\partial t})_j = \frac{\partial \frac{\rho}{2}(u^2 + v^2)}{\partial t} \approx \rho u(\frac{\partial u}{\partial t})_j + \rho v(\frac{\partial v}{\partial t})_j, \tag{8}$$

where $k = \frac{\rho}{2}(u^2 + v^2)$ denotes the (diagnostic) resolved-scale kinetic energy and the index j denotes any of the different processes so that $j = d, t, m, s$ refer to dynamics, turbulence, MSO or SSO parametrizations, respectively.

These results tell about the interactions between the different parametrization schemes that have also been noted earlier e.g. by Rontu et al. (2002); Rontu and Bazile (2003); Rontu (2004), see also Kim and Hogan (2004) for a global model. Turbulence parametrizations tend to compensate the effects of the SSO and MSO parametrizations so that the total drag due to all processess remains practically unchanged. The mission of a turbulence parametrization scheme in a NWP model is to smooth subgrid-scale vertical gradients independently of their origin or scale. SSO and MSO parametrizations, each with its own horizontal and vertical scale, tend to create such gradients. In this respect, compensation could be expected. In addition, differences of kinetic energy tendencies at upper levels (lower panel of Fig. 2) are due to modifications in the turbulence scheme, introduced

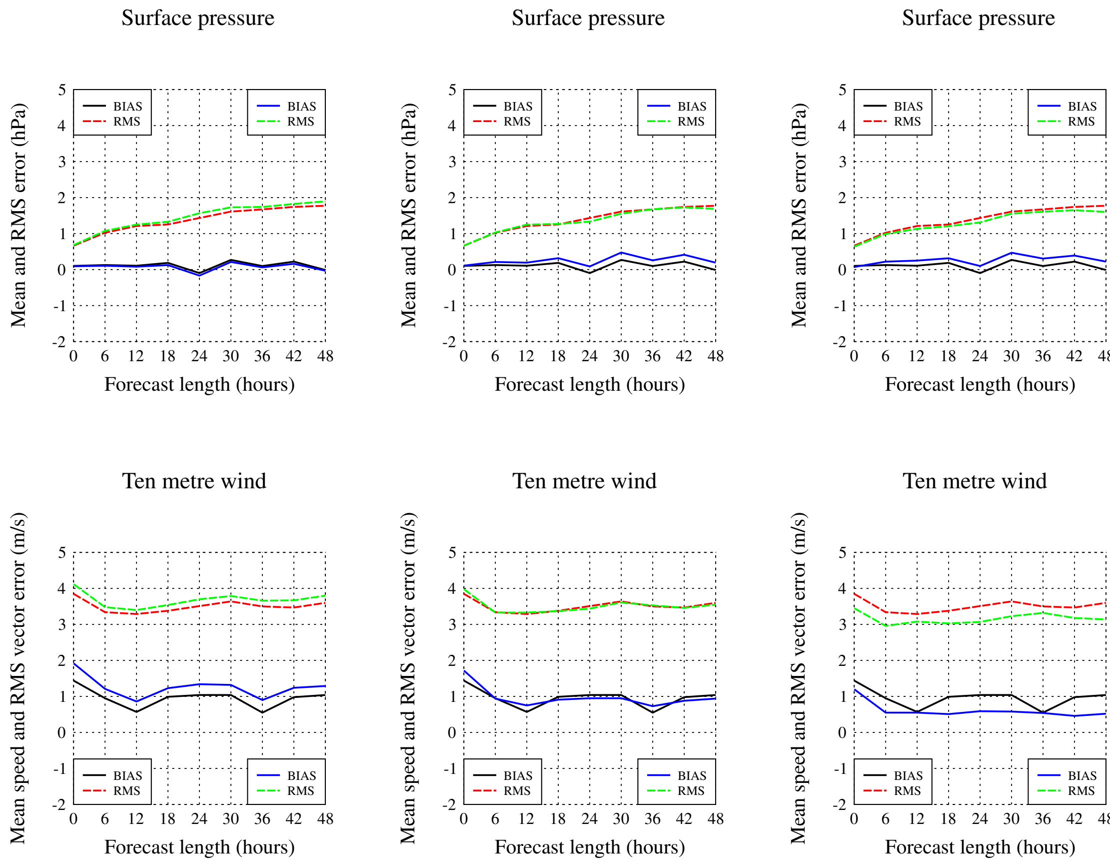

Figure 1: *Bias (solid) of* p_{msl} *(top) and ten-metre wind (bottom) and RMS error (dashed) from left to right: RC33 and NO33; RC33 and NM33; RC33 and NT33. The first experiment in each pair is shown with black and red, the second in blue and green. Please look at the coloured version of the report at http://hirlam.knmi.nl*

together with the rotated stress vector (see discussion in Tijm (2004)). This again points to the importance of formulation of the basic turbulence parametrizations.

Finally, averaged over time and Scandinavian area magnitudes of the surface stress due to the different parametrizations were calculated as a function of forecast length for the experiments NM33 and NT33 (not shown). In both cases, the magnitude of the turbulent component of the stress decreased towards the longer forecasts. This was shown to be due to the decrease of its y-component. No explanation for this behaviour was found and the limited sample of verification data does not allow making firm conclusions.

5 Summary

Parametrizations of the orography-related momentum fluxes in HIRLAM were renewed by replacing the orographic roughness by new meso- and small-scale orography parametrizations. The needed scale-dependent orography variables were derived from a high-resolution digital elevation data base.

Three series of parallel experiments were run. Verification results of ten-metre wind show similar or slightly improved quality in comparison with the reference HIRLAM. Behaviour of the turbulence scheme and its modifications may influence the results significantly. An analysis of the kinetic energy budgets shows, that parametrization schemes representing different sub-grid scales interact and partly compensate each other. New parametrizations increase the total drag only a little.

References

Beljaars, A. C. M., A. R. Brown, and N. Wood, 2004: A new parametrization of turbulent orographic form drag. *QJRMS*, **130**, 1327–1347.

Brown, A. R., and N. Wood, 2001: Turbulent form drag on anisotropic three-dimensional orography. *Bound. Lay. Met.*, **101**, 229–241.

Kim, Y.-J., and T. F. Hogan, 2004: Response of a global atmospheric model to various drag parametrizations. *Tellus*, **56A**, 472–484.

Mason, P., 1985: On the parameterization of the orographic drag. Technical report, Proc. Seminar on Physical parametrization for numerical models of the atmosphere. ECMWF, 139-165.

Rontu, L., 2003: Derivation of orography-related climate variables for a fine resolution hirlam. *HIRLAM Newsletter*, (44), 83–96, Available at http://hirlam.knmi.nl.

Rontu, L., 2004: Experimenting with the orography of hirlam. *HIRLAM Newsletter*, (45), 141–146, Available at http://hirlam.knmi.nl.

Rontu, L., and E. Bazile, 2003: Problems of mso parametrization: a case study with arpege-hirlam comparison. HIRLAM Workshop on Mesoscale Modelling, Dublin, 14 to 16 October 2002. Available at http://hirlam.knmi.nl.

Rontu, L., K. Sattler, and R. Sigg, 2002: Parametrization of subgrid-scale orography effects in HIRLAM. Technical Report 56, HIRLAM, 46pp. Available at http://hirlam.knmi.nl.

Sass, B. H., and N. W. Nielsen, 2004: Modelling of the hirlam surface stress direction. *HIRLAM Newsletter*, (45), 105–112, Available at http://hirlam.knmi.nl.

Tijm, A. B. C., 2004: Tuning CBR. *HIRLAM Newsletter*, (45), xx–yy, Available at http://hirlam.knmi.nl.

Undén, P., L. Rontu, H. Järvinen, P. Lynch, J. Calvo, G. Cats, J. Cuxart, K. Eerola, C. Fortelius, J. Garcia-Moya, C. Jones, A. McDonald, R. McGrath, B. Navascues, V. Ødegaard, E. Rodriguez, and *et al.*, 2002: The HIRLAM-5 scientific documentation december 2002. Available at http://hirlam.knmi.nl.

Wilson, J. D., 2003: Representing drag on unresolved terrain as a distributed momentum sink. *J. Atm. Sci.*, **99**, 1629–1637.

Wood, N., A. R. Brown, and F. E. Hewer, 2001: Parametrizing the effects of orography on the boundary layer: An alternative to effective roughness lengths. *Quart. J. Roy. Met. Soc.*, **127**, 759–777.

Wood, N., and P. Mason, 1993: The pressure force induced by neutral, turbulent flow over hills. *Quart. J. Roy. Met. Soc.*, **119**, 1233–1267.

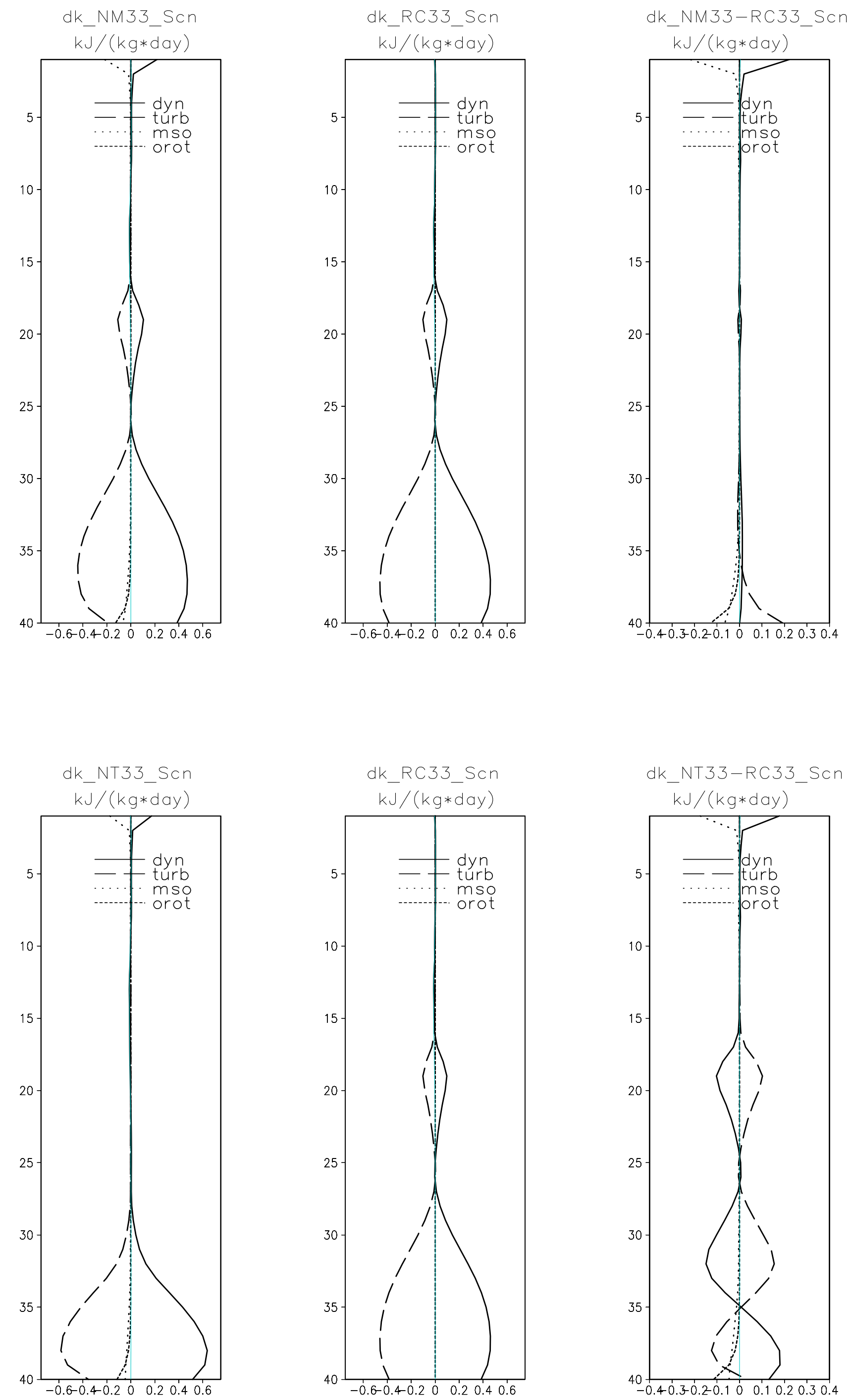

Figure 2: *Area- and time-averaged resolved scale kinetic energy tendencies due to model dynamics (dyn), parametrized turbulence (turb), meso-scale orography (mso) and small-scale orography (orot) from experiments RC33 compared to NM33 (upper panel) and to NT33 (lower panel). Unit 1000*m^2s^{-2}*/day (left and middle) and* m^2s^{-2}*/day (right, note the different horizontal scales in the figures.). Vertical axis: model level from bottom to top. In this figure, every model layer gets equal weight in spite of the different thicknesses of the layers.*